Available online at www.sciencedirect.com
SCIENCE DIRECT®
Journal of the European Ceramic Society 25 (2005) 55–63
www.elsevier.com/locate/jeurceramsoc

Hard, tough and strong ZrO_2–WC composites from nanosized powders

Guy Anné, Stijn Put, Kim Vanmeensel, Dongtao Jiang, Jef Vleugels*, Omer Van der Biest

Department of Metallurgy and Materials Engineering (MTM), K.U. Leuven, Kasteelpark Arenberg 44, B-3001 Heverlee, Belgium

Received 10 November 2003; received in revised form 19 January 2004; accepted 25 January 2004
Available online 19 May 2004

Abstract

Yttria-stabilised zirconia (Y-TZP) based composites with a tungsten carbide (WC) content up to 50 vol.% were prepared from nanopowders by means of conventional hot pressing. The mechanical properties were investigated as a function of the WC content. The hardness increased from 12.3 GPa for pure Y-TZP up to 16.4 GPa for the composite with 50 vol.% WC, whereas the bending strength reached a maximum of 1551 MPa for the 20 vol.% WC composite. The toughness of the composites could be optimised by judicious adjustment of the overall yttria content by mixing monoclinic and 3 mol% Y_2O_3 co-precipitated ZrO_2 starting powders. An optimum fracture toughness of 9 MPa $m^{1/2}$ was obtained for a 40% WC composite with an overall yttria content of 2 mol%. The hardness, strength as well as fracture toughness of the ultrafine grained composites with a nanosized WC source was significantly higher than with micron-sized WC. The experimentally measured contribution of the different observed toughening mechanisms was evaluated as a function of the WC content. Transformation toughening was found to be the major toughening mechanism in ZrO_2–WC composites with up to 30 vol.% WC, whereas the contribution of crack deflection and bridging is significant at a secondary phase content above 30 vol.%.

Keywords: Hot pressing; Composites; Mechanical properties; Toughness; ZrO_2–WC; WC

1. Introduction

Tetragonal zirconia polycrystalline (TZP) materials have excellent mechanical properties such as a high bending strength and excellent fracture toughness, due to transformation toughening.[1] The modest hardness of these materials however limits their use for wear applications.

During the last decade, the applicability of zirconia to induce transformation toughening of non-oxide materials by the martensitic stress-induced transformation of tetragonal ZrO_2 (t-ZrO_2) to monoclinic ZrO_2 (m-ZrO_2) was investigated. Amongst the composite systems investigated are mullite–ZrO_2,[2] Si_3N_4–ZrO_2,[3] TiB_2–ZrO_2[4–7] and Ti(C, N)–ZrO_2.[8,9] Other reported systems in which the ZrO_2 is present as the matrix phase includes ZrO_2–Al_2O_3–TiC,[10] ZrO_2–SiC,[11] ZrO_2–Cr_2O_3, ZrO_2–Cr_3C_2 and ZrO_2–Cr_7C_3.[12] Recently, ZrO_2-based composites with hard TiB_2, TiCN, TiN and TiC secondary phase additions were described.[13] Although excellent toughness values could be achieved with an yttria-coated ZrO_2 starting powder, the increase in hardness aimed at by the addition of the hard secondary phases was rather modest.[13] The addition of micron-sized WC grains to a ZrO_2 matrix was reported to increase the hardness significantly, although the reported toughness values were rather low.[14–16] The major toughening mechanisms in the ZrO_2–WC composites investigated were identified to be microcracking, crack bridging, crack deflection and crack branching.[17]

In this paper, ZrO_2–WC composites were prepared from nanopowders. Their mechanical properties are evaluated and a route to optimise the fracture toughness of the composites is described. Moreover, the contribution of the individual toughening mechanisms to the total toughness of the composites is elucidated.

* Corresponding author. Tel.: +32-16-321244; fax: +32-16-321992.
E-mail address: jozef.vleugels@mtm.kuleuven.ac.be (J. Vleugels).

0955-2219/$ – see front matter © 2004 Elsevier Ltd. All rights reserved.
doi:10.1016/j.jeurceramsoc.2004.01.015

2. Experimental procedure

Two WC powder sources were used. Eurotungstene grade CW5000 with an average particle size of 0.8–1 μm and Nanodyne grade Nanocarb WC/Co12. The latter starting powder consists of about 50 μm large WC/Co composite agglomerates with individual WC crystals claimed to be in the range 20–40 nm. The Co was leached out in HCl at 50 °C. After leaching, the powder was washed with distilled water to remove the chlorides. Final washing was done in iso-propanol to obtain soft WC agglomerates. The washed powder was subsequently dried at 90 °C for 12 h. The effect of the cobalt leaching and additional milling with WC/Co balls in iso-propanol for 48 h on the Nanocarb WC/Co12 are illustrated in Fig. 1. The agglomerates of the original composite powder disintegrated in finer agglomerates due to the removal of the Co binder. Subsequent Turbula mixing in iso-propanol using hardmetal milling balls (∅ = 4–5 mm, CERATIZIT grade MG15) for 48 h resulted in submicron nanoparticle agglomerates, as shown in Fig. 1c. Even though contrast between individual WC crystals is poor, WC platelets with a diameter of up to 150 nm can be recognised in these agglomerates. The ZrO_2 powders are commercially available powders, i.e., pure monoclinic (Tosoh grade TZ-0) and 3 mol% Y_2O_3 co-precipitated (Daiichi grade HSY-3U) ZrO_2 nanopowders. The crystal size of both powders is

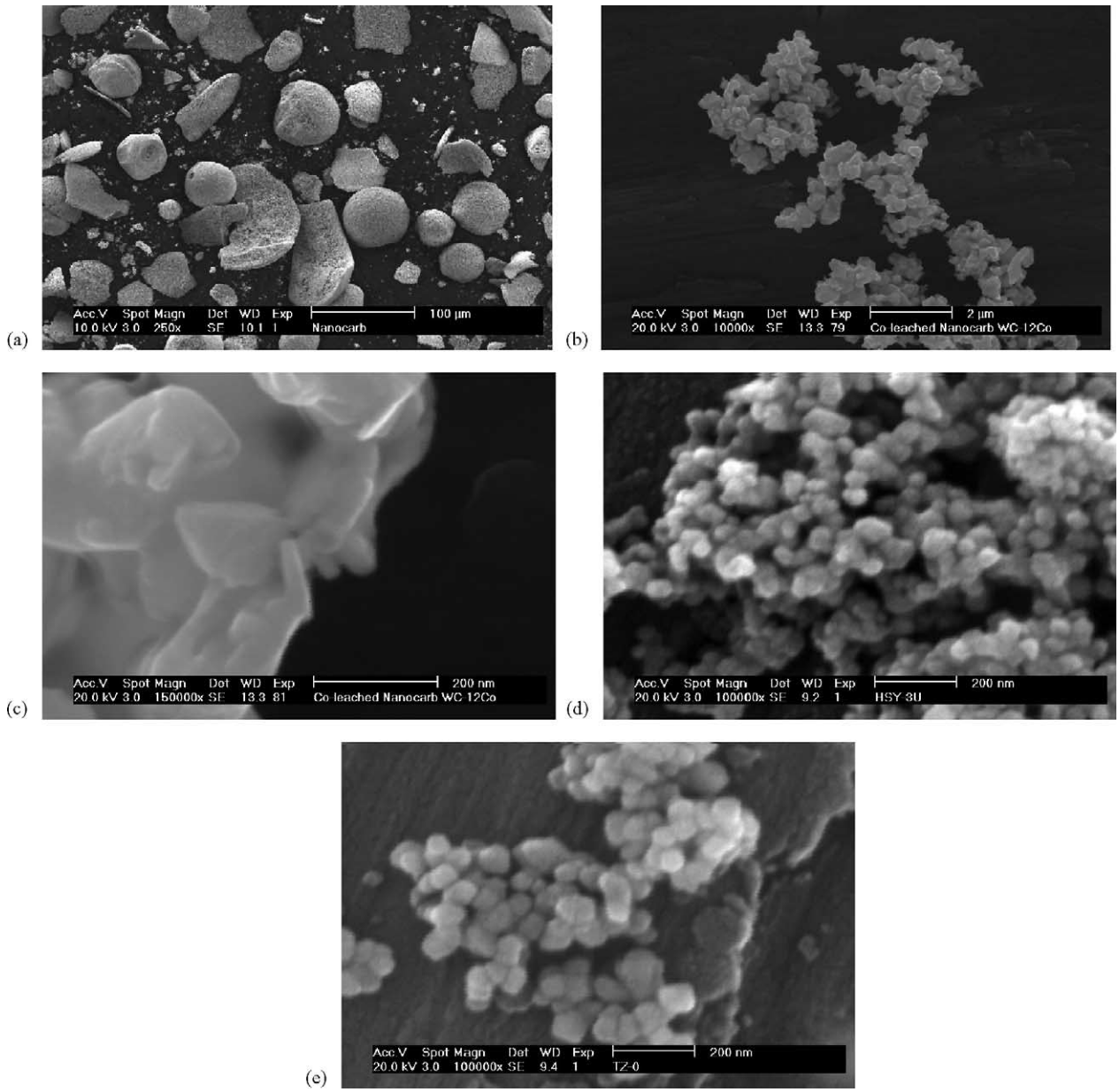

Fig. 1. Original Nanocarb WC/Co powder agglomerates (a), WC grains after Co-leaching and mixing for 24 h in iso-propanol (b and c), and the 3 mol% Y_2O_3 stabilised (TZ-3Y) (d), and monoclinic (TZ-0) (e), ZrO_2 starting powders.

Table 1
Starting powders

Powder	Grade	Supplier	Powder size[a]
ZrO_2	HSY-3U (3 mol% yttria)	Daiichi	30 nm (crystals)
ZrO_2	TZ-0	Tosoh	27 nm (crystals)
WC	CW5000	Eurotungstene	0.8–1.0 μm
WC	Nanocarb (WC/Co12)	Umicore/ Nanodyne	Agglomerate size 49 μm crystal size 20–40 nm

[a] According to the suppliers' data sheets.

around 30 nm, as shown in Fig. 1d and e. Powder mixtures with an Y_2O_3-content between 1.75 and 3.00 mol% were obtained by mixing both ZrO_2 starting powders in the appropriate ratio. An overview of the starting powders is given in Table 1.

For the preparation of the composites, 60 g of powder was mixed on a multidirectional mixer (type Turbula) in iso-propanol in a polyethylene container of 250 ml during 48 h. Three hundred grams of pure alumina balls with a diameter of 10 mm were added to the container to break the agglomerates during mixing. After mixing, the iso-propanol was removed by means of a rotating evaporator. The dry powder mixture was inserted into a graphite container with a diameter of 30 mm, coated with boron nitride. After cold compression at 30 MPa, the samples were hot pressed in a KCE hot press (W 100/150-2200-50 LAX, FCT Systeme der Strukturkeramik, Rauenstein, Germany) in vacuum (≈0.1 Pa) under a mechanical load of 28 MPa. The samples were separated from the furnace atmosphere by the graphite hot press set-up, where the sliding contacts were sealed by boron nitride. The ceramic samples were hot pressed for 1 h at 1450 °C, with a heating rate of 50 °C/min and a cooling rate of 10 °C/min.

The Vickers hardness, H_{V5}, H_{V10} and H_{V30}, was measured on a Zwick hardness tester (model 3202, Zwick, Ulm, Germany) with an indentation load of 5, 10 and 30 kg, respectively. The reported values are the mean of at least five indentations. The indentation fracture toughness, K_{Ic}, was calculated from the length of the radial cracks. The reported values are the mean and standard deviation of at least five indentations. The fracture toughness was calculated according to the formula of Anstis et al.[18] The elastic modulus, E, of the ceramic specimens was measured by the resonance frequency method.[19] The resonance frequency was measured by the impulse excitation technique (Grindo-Sonic, J.W. Lemmens N.V., Leuven, Belgium). The density of the specimens was measured in ethanol, according to the Archimedes method. The flexural strength at room temperature was measured in a 3-point bending test (Series IX Automated Materials Testing System 1.29, Instron Corporation) on rectangular (25.0 mm × 5.4 mm × 2.1 mm (height)) specimens with a span width of 20 mm and a crosshead displacement of 0.1 mm/min. All surfaces were ground with a diamond grinding wheel (type MD4075B55, Wendt Boart, Brussels, Belgium). The reported values are the mean and standard deviation of at least five bending tests.

For microstructural investigation, a SEM (XL30FEG, FEI Company, Eindhoven, The Netherlands) was used. X-ray diffraction analysis (XRD, 3003-TT, Seifert, Ahrensburg, Germany) using Cu Kα radiation (40 kV, 30 mA) was used for phase identification and determination of the relative phase contents. For the calculation of the monoclinic and tetragonal phase content, the method of Toraya was used.[20]

In selected composites, a comparison of the transformability of the tetragonal zirconia, defined as the fraction that can be transformed into monoclinic ZrO_2, was obtained by measuring the difference in monoclinic phase content on polished and on fractured surfaces, obtained by breaking a sample in a 3-point bending test.

3. Results

Microstructural investigation of the hot pressed ZrO_2–WC composites revealed that full densification could be achieved after 1 h at 1450 °C. Homogeneous ZrO_2–WC microstructures were obtained after 48 h of mixing of the starting powders. Some representative backscattered electron micrographs are shown in Fig. 2. Three phases can be clearly differentiated, i.e., ZrO_2 (grey), WC (white) and Al_2O_3 (black). The Al_2O_3 grains originated from the alumina mixing medium. X-ray fluorescence analysis revealed the alumina content to be around 2 vol.% in the ZrO_2–WC composites. Although grain growth of the Nanocarb WC phase during sintering is obvious comparing Fig. 1c with Fig. 3c and d, the final grain size of the WC phase in the Nanocarb powder based composites is smaller than that in the micron-sized powder based. The grain growth of the WC nanopowder might be attributed to the presence of a residual amount of Co, that was determined to be 0.75 wt.% (relative to the WC content) by means of X-ray fluorescence. Co and WC form a eutectic around 1290 °C, what is clearly below the actual hot pressing temperature. The backscattered electron micrographs of the fracture surface of the Nanocarb and CW5000 WC powder based ZrO_2–WC (60/40) composites, presented in Fig. 3, reveal that the WC distribution is better in the nanopowder-based material, resulting in a larger fraction of ultrafine WC particles in the 100–200 nm range. The angular geometry of the WC grains remained after sintering, indicating that the ZrO_2 and WC phases are chemically compatible at the sintering temperature. The fracture mode for both ZrO_2 and WC phases is intergranular. The maximum grain size of the WC grains in the ZrO_2–WC (80/20) composite is well below 1 μm. At WC contents above 20 vol.%, the WC grains tend to agglomerate in small clusters. WC network formation is obvious at WC contents above 40%.

Since the fracture toughness of Y-TZP materials can be modified by adjusting the Y_2O_3 stabiliser content, the influence of changing the overall yttria content on the fracture

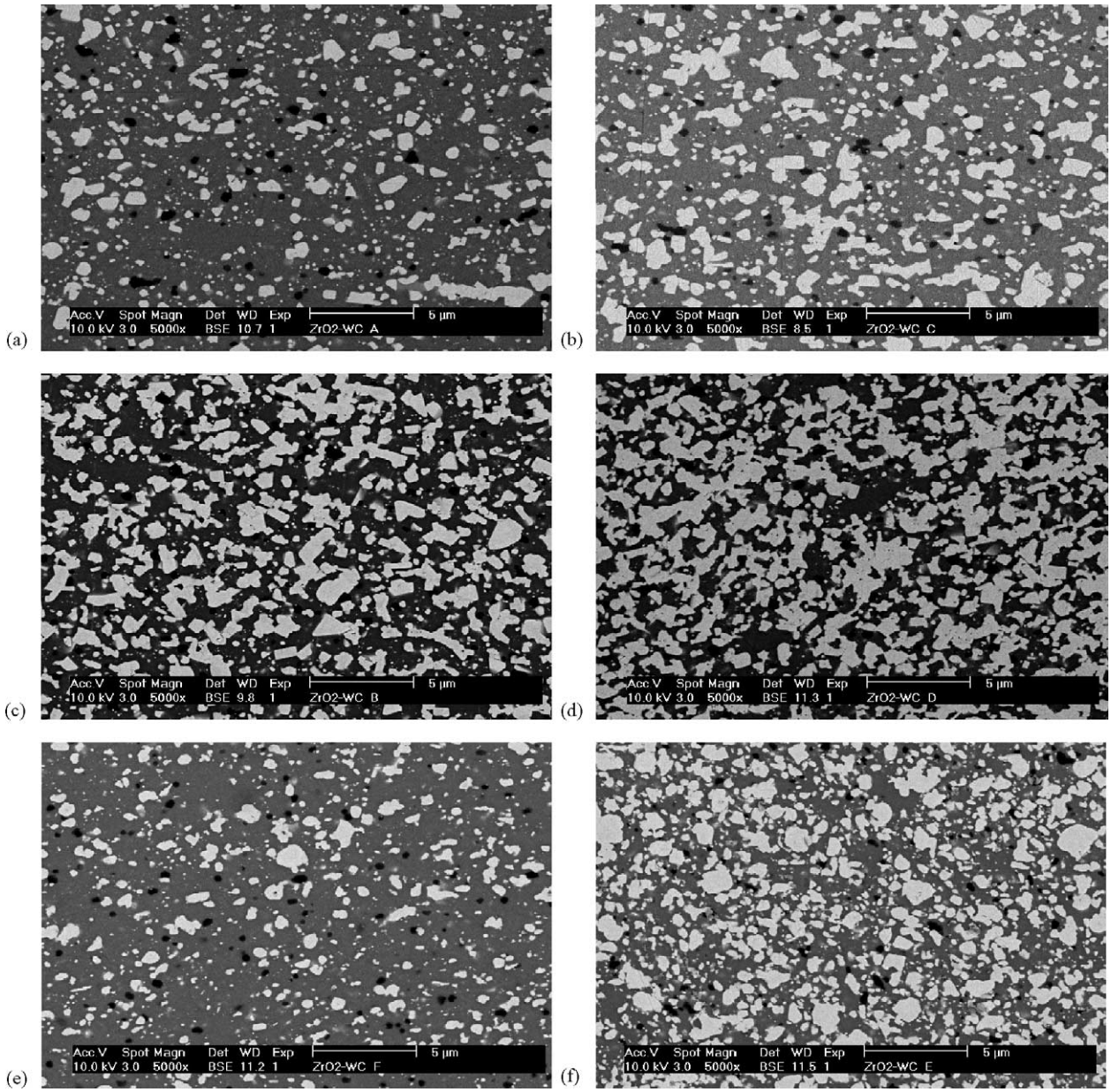

Fig. 2. Backscattered electron micrographs revealing the microstructure of 20 vol.% (a), 30 vol.% (b), 40 vol.% (c) and 50 vol.% (d) Nanocarb WC grade and 20 vol.% (e) and 40 vol.% (f) CW5000 WC grade Y-TZP/WC composites. The phases that can be differentiated are WC (white), ZrO_2 (grey) and Al_2O_3 (black).

toughness was investigated for ZrO_2–WC (60/40) composites. The change in overall yttria content was established by mixing the pure monoclinic and 3 mol% yttria-stabilised ZrO_2 powders in the appropriate amount, an approach that has proven to be very effective in optimising the fracture toughness of Y-TZP ceramics.[21] The obtained results, given in Table 2, clearly reveal that the fracture toughness of the composites increases with decreasing yttria content from 3 to 2 mol%. At an overall yttria content of 1.75 mol% however, the ZrO_2 phase in the samples spontaneously transforms to m-ZrO_2 upon cooling after sintering, resulting in macrocracking of the hot pressed material. An excellent fracture toughness of 9.2 MPa $m^{1/2}$ was obtained for the 2Y-TZP-WC (60/40) composite. The hardness of the composites was hardly influenced by a reduction of the yttria content down to 2 mol%, whereas the *E*-modulus decreased with decreasing yttria content.

Because of the excellent fracture toughness obtained with the 2Y-TZP based composites, this matrix was selected to further investigate the influence of the amount and size of the WC phase. The density, *E*-modulus, hardness, toughness and flexural strength of 2 mol% Y_2O_3-stabilised ZrO_2-WC composites are summarised in Table 3. The hardness and fracture toughness of the Nanocarb WC grade powder

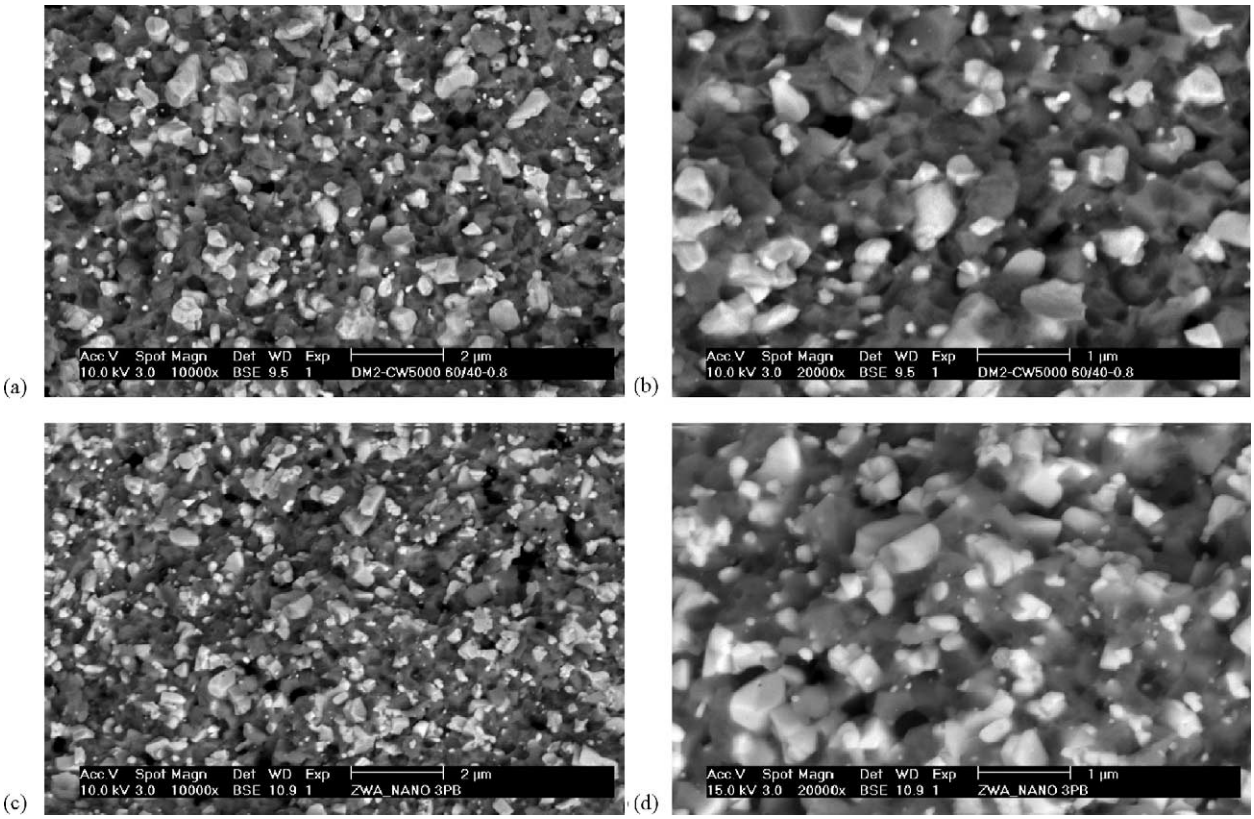

Fig. 3. Backscattered electron micrographs of fracture surfaces of the CW5000 (a and b) and Nanocarb (c and d) WC powder based ZrO_2–WC (60/40) composites. The phases that can be differentiated are WC (white) and ZrO_2 (grey).

based composites are graphically illustrated in Fig. 4. The hardness of the composites was strongly influenced by the WC content and increased linearly with increasing WC content from 12.28 GPa (H_{V10}) for the Y-TZP ceramic up to 16.40 GPa for the 50 vol.% WC composite. The hardness of the 40 vol.% WC nanopowder-based composite is about 2.50 GPa higher than that of the micron-sized powder based composite, whereas the hardness of the 20 vol.% ZrO_2–WC composites is comparable for both WC powders.

Table 2
Mechanical properties of Y-TZP/WC composites with 40 vol.% nanosized WC starting powder and varying Y_2O_3 content

Y_2O_3 (mol%)	ρ (g/cm^3)	E (GPa)	H_{V10}[a] (GPa)	K_{Ic10}[a] (MPa m$^{1/2}$)
2.00	9.99	322	15.16 ± 0.20	9.2 ± 0.3
2.50	9.90	353	15.70 ± 0.20	6.5 ± 0.3
3.00	9.94	378	15.13 ± 0.19	6.0 ± 0.2

[a] Mean and standard deviation of at least five indentations.

Table 3
Mechanical properties of 2Y-TZP/WC composites as a function of WC phase content

WC grade	WC (vol.%)	E (GPa)	ρ (g/cm^3)	H_{V10}[a] (GPa)	K_{Ic10}[a] (MPa m$^{1/2}$)	Strength (MPa)[a]
–	0	203	6.06	12.28 ± 0.11	10.1 ± 0.1	1258 ± 114
Nanocarb	20	268	8.13	13.33 ± 0.06	9.9 ± 0.3	1551 ± 16
Nanocarb	30	265	9.03	14.01 ± 0.06	9.2 ± 0.2	1303 ± 89
Nanocarb	40	322	9.99	15.16 ± 0.20	9.2 ± 0.3	1036 ± 87
Nanocarb	50	365	10.71	16.40 ± 0.44	8.1 ± 0.3	488 ± 49
CW5000	20	259	7.93	13.50 ± 0.23	8.7 ± 0.3	1360 ± 85
CW5000	40	304	9.95	13.56 ± 0.29	7.9 ± 0.2	903 ± 64

[a] Mean and standard deviation of at least five indentations or bending bars.

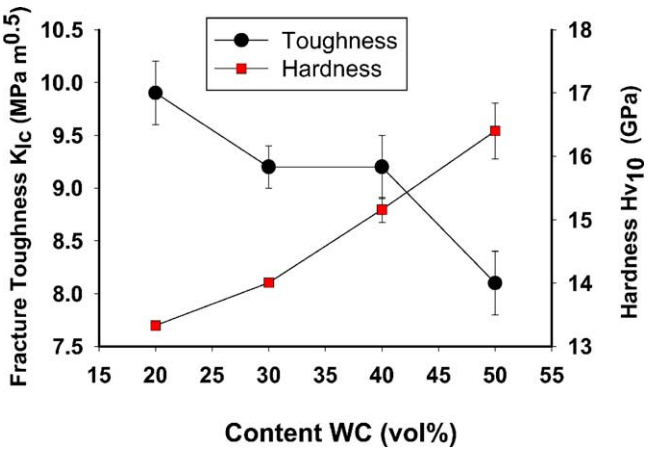

Fig. 4. Fracture toughness.

Beside the high hardness, excellent toughness values of more than 8 MPa $m^{1/2}$ were obtained. For the 2Y-TZP and ZrO_2–WC (80/20) composite, the toughness was as high as 10 MPa $m^{1/2}$. The toughness of the ZrO_2–WC (70/30) and (60/40) composites was comparable, i.e., 9.2 MPa $m^{1/2}$. The toughness of the ZrO_2–WC (50/50) composite was 8.2 MPa $m^{1/2}$. The fracture toughness of the composites with the nominally nanograined WC is higher than that of the composites with micron-sized WC.

Excellent flexural strengths, well above 1 GPa, were obtained for the ZrO_2–WC composites with up to 40 vol.% WC, as illustrated for the 2Y-TZP based composites in Fig. 5. A maximum strength of 1551 ± 16 MPa was obtained for the composite with 20 vol.% of WC nanopowder, which is well above the bending strength of the pure 2Y-TZP, being 1258 MPa. It should also be clear that the flexural strength of the WC nanopowder based composites is about 200 MPa higher than for the composites with micron-sized WC starting powder.

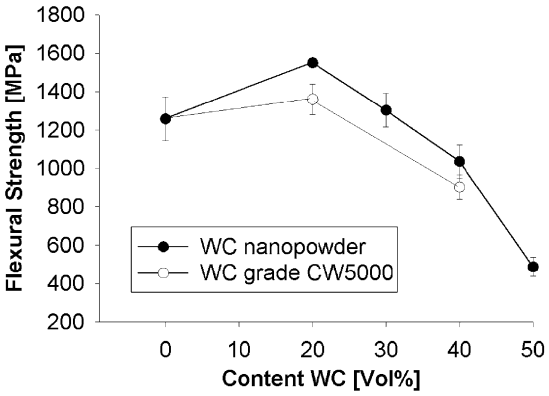

Fig. 5. Flexural strength of 2Y-TZP/WC composites, with WC nanopowder and WC grade CW5000.

4. Discussion

Unlike in other Y-TZP composite systems with TiB_2, TiN, TiC or TiCN additions, where the hardness is rather modest (H_{V10} = 12–13 GPa) and hardly influenced by the amount of secondary phase content up to 40 vol.%,[13] the hardness in the ZrO_2–WC system clearly increases with increasing WC content. The high hardness in the ZrO_2–WC composites can be explained by the good coherence between WC and the ZrO_2 matrix[22] and the chemical compatibility of WC and ZrO_2,[23] whereas the Ti-based additives were found to partially dissolve in the ZrO_2 matrix[13] and reaction products can develop.[24]

Beside the volume fraction of the WC in the composites, the size of the WC particles strongly influences the hardness of the composites. For the composites with 40 vol.% WC, the composite with the micron-sized CW5000 powder had a hardness of 13.56 GPa, whereas the hardness of the composites with the nanosized WC starting powder was significantly higher, i.e., 15.16 GPa, as summarised in Table 3. The use of finer WC starting powder clearly results in higher hardness values for the ZrO_2–WC composites and is also responsible for the higher flexural strengths, as shown in Fig. 5.

In the present investigation, the indentation toughness method was chosen as it is an easy and effective way to make a ranking of the materials based on their toughness. The observed indentation crack profiles closely follow the well-established radial or Palmqvist crack pattern. Therefore, the indentation toughness data are thought to be reliable as far as ranking of the investigated materials is concerned. The toughness measured by the conventional indentation technique is reported to be lower than that of the long crack toughness of transformation toughened materials.[1] This is due to the fact that the conventional indentation theory neglects the effect of stress induced transformation on the volume expansion of the plastic zone beneath the indentation, that forms an additional driving force for the indentation cracking in materials containing transformable phase. In order to check for "R-curve" effects, the indentation toughness was measured for different crack lengths by increasing the indentation load. The measured hardness and toughness values, obtained with an indentation load of at 5, 10 and 30 kg, are given in Table 4.

For the 2Y-TZP/WC (Nanocarb) grades, the indentation toughness is found to have reached the steady state value even with an indentation load of 5 kg. It is also clear from the data presented in Table 4 that the relative ranking of the investigated Y-TZP materials in terms of indentation toughness is the same, irrespective of the indentation loads.

Additional information on the transformability of the ZrO_2 matrix in the optimised 2Y-TZP based composites could be obtained from XRD analysis of polished and fractured ceramic surfaces. The m-ZrO_2 fraction on polished and fractured materials is listed in Table 5. The reported values were obtained from at least five surfaces. The transformability of the zirconia phase, defined as the fraction

Table 4
Hardness and toughness of 2Y-TZP/WC (Nanocarb) composites as a function of the indentation load

WC (vol.%)	H_{V5} (GPa)	H_{V10} (GPa)	H_{V30} (GPa)	K_{Ic5} (MPa m$^{1/2}$)	K_{Ic10} (MPa m$^{1/2}$)	K_{Ic30} (MPa m$^{1/2}$)
20	13.45 ± 0.22	13.33 ± 0.06	13.35 ± 0.12	9.7 ± 0.6	9.9 ± 0.3	10.1 ± 0.8
30	14.11 ± 0.15	14.01 ± 0.06	13.95 ± 0.15	9.0 ± 0.2	9.2 ± 0.2	9.0 ± 0.4
40	15.11 ± 0.21	15.16 ± 0.20	14.86 ± 0.13	8.9 ± 0.1	9.2 ± 0.3	9.0 ± 0.4
50	16.49 ± 0.16	16.40 ± 0.44	16.17 ± 0.21	8.3 ± 0.2	8.1 ± 0.3	7.9 ± 0.3

The reported values are the mean and standard deviation of at least five indentations.

Table 5
2Y-TZP ZrO_2 phase and composite transformability

WC (vol.%)	$V_m^{fractured}$ [a] (%)	$V_m^{polished}$ [a] (%)	ZrO_2 phase transformability (%)	$M^{fractured}$ [b] (vol.%)	$M^{polished}$ [b] (vol.%)	Composite transformability (%)
0	71 ± 2	8.4 ± 0.6	63 ± 2	71 ± 2	8.4 ± 0.6	63 ± 2
20	67 ± 4	6.5 ± 0.8	61 ± 1	53 ± 3	3.3 ± 0.5	51 ± 1
30	60 ± 1	7.2 ± 0.9	53 ± 1	42 ± 1	3.6 ± 0.5	38 ± 1
40	54 ± 2	8.5 ± 0.4	46 ± 2	33 ± 1	4.2 ± 0.3	28 ± 1
50	49 ± 2	7.9 ± 0.8	41 ± 2	25 ± 1	3.9 ± 0.4	21 ± 1

[a] m-ZrO_2 fraction of the ZrO_2 matrix measured on polished and fractured surfaces.
[b] vol.% m-ZrO_2 in the composite, measured on polished and fractured surfaces.

of the ZrO_2 matrix that can be transformed into m-ZrO_2 upon fracturing, can be calculated from the m-ZrO_2 phase content measured on fractured and polished surfaces. The transformability of the composite is defined as the volume percent of t-ZrO_2 in the composite as a whole that transforms during fracturing. The t-ZrO_2 and composite transformability is plotted as a function of the WC content for the 2Y-TZP based materials in Fig. 6. The transformability of the tetragonal zirconia phase decreased from 63% in the pure 2Y-TZP down to 41% in the composite with 50 vol.% WC, as shown in Table 5. Accordingly, the transformability of the composite decreases with increasing WC content. The reduced transformability can be attributed to the increasing WC phase content, reducing the size of the transformation zone around propagating cracks.

Beside transformation toughening, scanning electron microscopy investigation of the radial crack pattern originating at the corners of Vickers indentations revealed that propagating cracks were deflected by the WC grains, as shown in Fig. 7a and b for respectively the 80/20 and 60/40 composite. Microcracks, crack branching and crack bridging were not observed at the crack front. In literature however, the major toughening mechanisms in ZrO_2–WC composites were identified to be microcracking, crack bridging, crack deflection and crack branching.[17]

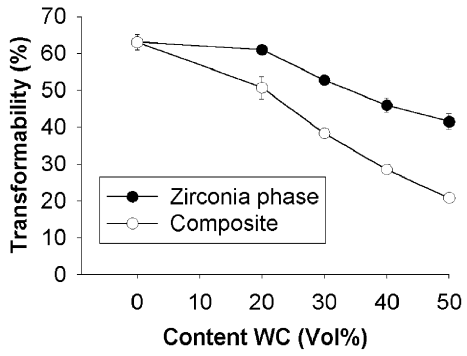

Fig. 6. ZrO_2 phase and composite transformability of 2Y-TZP/WC composites with varying WC content.

The overall toughness of the composites can be described as:

$$K_{Ic} = K_0 + \Delta K_C \quad (1)$$

where K_0 is the toughness of the non-transforming matrix and ΔK_C is the contribution of the different active toughening mechanisms. Based on the observed mechanisms in the 2Y-TZP/WC composites, this can be rewritten as:

$$\Delta K_C = \Delta K_{cT} + \Delta K_{cD} + \Delta K_{cB} \quad (2)$$

where ΔK_{cT} is the contribution from transformation toughening, ΔK_{cD} is the crack deflection contribution and ΔK_{cB} is the contribution of other active toughening mechanisms.

The experimentally measured indentation fracture toughness, K_{Ic} (10 kg), of a non-transformable Daiichi grade HSY-3U powder, hot pressed for 1 h at 1450 °C, was 3.5 ± 0.1 MPa m$^{1/2}$. An experimental value which is very close to the reported matrix toughness, K_0 = 3.3 MPa m$^{1/2}$ for Y-TZP ceramics.[1,25]

From the measured fracture toughness of 10.1 MPa m$^{1/2}$ and a measured ZrO_2 phase transformability of 63% for the pure 2Y-TZP material, it is assumed that this transformability corresponds to a toughness increase of 6.6 MPa m$^{1/2}$ above the baseline matrix toughness of 3.5 MPa m$^{1/2}$. For the composites, the effective contribution of transformation toughening is scaled down in proportion to the measured composite transformability shown in Table 5. In all cases,

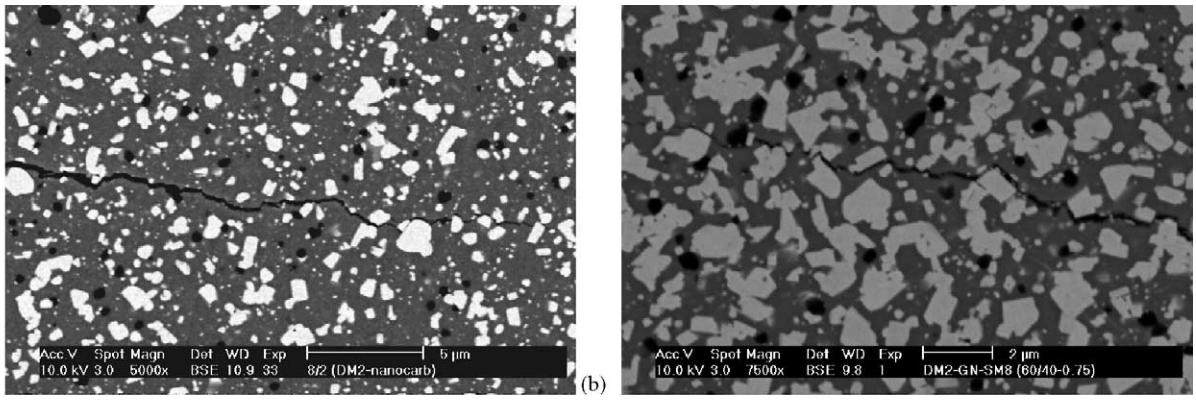

Fig. 7. Backscattered electron micrographs revealing crack deflection (a and b) and crack bridging (b) by the WC grains in the composites with 20 vol.% (a) and 50 vol.% (b) of WC.

the actual toughness is still higher and this additional toughness is attributed to other toughening mechanisms. The results of this analysis are graphically presented in Fig. 8.

From Fig. 8, it is clear that transformation toughening is the primary toughening mechanism in the composites with 20 and 30 vol.% WC. The matrix toughness, transformation toughening and toughening by combined crack deflection and other toughening mechanisms are equally important in the ZrO_2–WC (60/40) composites with 40 and 50 vol.% WC. The importance of the crack deflection mechanism increases with increasing WC content. The crack deflection model of Faber and Evans[26] predicts a toughness increase of 15% for ceramic composites with 30 vol.% of spherical secondary phase particles, which is in excellent agreement with the observations for the ZrO_2–WC (70/30) composite. Indeed, the calculated toughness increase through crack deflection accounts for 18% in the ZrO_2–WC (70/30) composites. An important feature of the crack deflection analysis by Faber and Evans[26] is the decreasing contribution of crack deflection at volume fractions in excess of 20 vol.%. This would imply that the experimentally observed (see Fig. 8) increased contribution of crack deflection with increasing WC content should be mainly attributed to other toughening mechanisms than crack deflection like crack bridging activity.

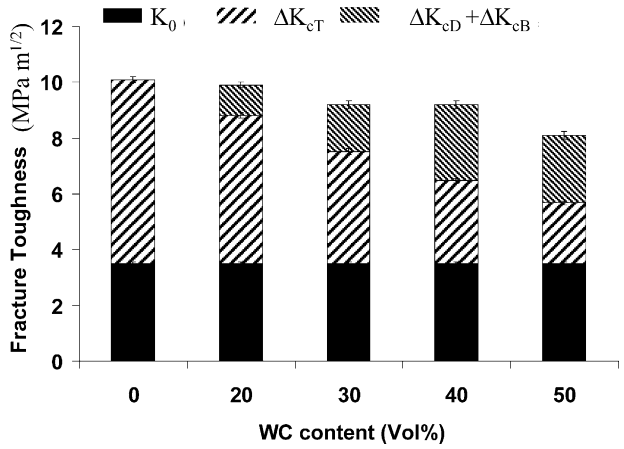

Fig. 8. Contribution of the observed toughening mechanisms to the fracture toughness of 2Y-TZP/WC composites. ΔK_{cT} = transformation toughening, ΔK_{cD} = crack deflection, ΔK_0 = toughness of the non-transformable ZrO_2 matrix and ΔK_{cB} = other toughening mechanisms.

5. Conclusions

Fully dense ZrO_2–WC composites with excellent toughness (>8 MPa $m^{1/2}$), hardness (>14.50 GPa) and bending strength (>1 GPa) were prepared from ZrO_2 and WC nanopowders by means of hot pressing at 1450 °C.

The hardness, strength and fracture toughness of the composites prepared with WC nanopowders was substantially higher than that of the micron-sized WC powder based ceramics.

Composites with optimum fracture toughness were obtained by engineering of the ZrO_2 matrix. A maximum toughness was achieved with an overall yttria stabiliser content of 2 mol%, established by mixing pure monoclinic and 3 mol% Y_2O_3 co-precipitated ZrO_2 starting powders.

Experimental observations allowed to evaluate the relative contribution of the matrix toughness, transformation toughening and combined crack deflection and bridging to the fracture toughness of the composites as a function of the WC content. Transformation toughening is important in all investigated composites with a WC content up to 50 vol.% and is the primary toughening mechanism in the composites up to 40 vol.% WC. The contribution of combined crack deflection and other toughening mechanisms increases with increasing WC content and becomes as important as the ZrO_2 matrix toughness and transformation toughening in the ZrO_2–WC (60/40) composites.

Acknowledgements

This work was supported by the Brite-Euram program of the Commission of the European Communities under project contract No. BRPR-CT97-0432.

References

1. Hannink, R. H. J., Kelly, P. M. and Muddle, B. C., Transformation toughening in zirconia-containing ceramics. *J. Am. Ceram. Soc.* 2000, **83**, 461–487.
2. Qi-Ming, Y., Jia-Qi, T. and Zheng-Guo, J., Preparation and properties of zirconia toughened mullite ceramics. *J. Am. Ceram. Soc*. 1986, **69**, 265–267.
3. Knutson-Wedel, M., Falk, L. K. L. and Ekström, T., Characterization of Si_3N_4 ceramics formed with different oxide additives. *J. Hard. Mater.* 1992, **3**, 435–445.
4. Telle, R., Meyer, S., Petzow, G. and Franz, E. D., Sintering behaviour and phase reactions of TiB_2 with ZrO_2 additives. *Mater. Sci. Eng.* 1988, **A105/106**, 125–129.
5. Telle, R. and Petzow, G., Strengthening and toughening of boride and carbide hard material composites. *Mater. Sci. Eng.* 1988, **A105/106**, 97–104.
6. Watanabe, T. and Shoubu, K., Mechanical properties of hot pressed TiB_2–ZrO_2 composites. *J. Am. Ceram. Soc.* 1985, **68**, C34–C36.
7. Shoubu, K., Watanabe, T., Drennan, J., Hannink, R. H. J. and Swain, M. V., Toughening mechanisms and microstructures of TiB_2–ZrO_2 composites. In *Advances in Ceramics, Vol 24*: *Science and Technology of Zirconia III*. American Ceramic Society, Columbus, 1988, pp. 1091–1099.
8. Gross, V., Haylock, J. and Swain, M. V., Transformation toughened titanium carbo-nitride zirconia composites. *Mater. Sci. Forum* 1988, **34–36**, 555–559.
9. Barbier, E. and Thevenot, F., Titanium carbonitide zirconia composites formation and characterisation. *J. Eur. Ceram. Soc*. 1991, **8**, 263–269.
10. Fukuhara, M., Properties of (Y)ZrO_2–Al_2O_3 and (Y)ZrO_2–Al_2O_3-(Ti or Si)C composites. *J. Am. Ceram. Soc*. 1989, **72**, 236–242.
11. Dougherty, S. E., Nieh, T. G., Wadsworth, J. and Akimune, Y., Mechanical properties of a 20 vol% SiC whisker-reinforced, yttria-stabilized, tetragonal zirconia composite at elevated temperatures. *J. Mater. Res.* 1995, **10**, 113–115.
12. Pêdzich, Z., Haberko, K., Babiarz, J. and Faryna, M., The TZP-chromium oxide and chromium carbide composites. *J. Eur. Ceram. Soc.* 1998, **5**, 1939–1943.
13. Vleugels, J. and Van der Biest, O., Development and characterization of Y_2O_3-stabilized ZrO_2 (Y-TZP) composites with TiB_2, TiN, TiC. *J. Am. Ceram. Soc.* 1999, **82**, 2717–2720.
14. Pêdzich, Z., Haberko, K. and Faryna, M., Tetragonal zirconia-tungsten carbide composites manufacturing, microstructure and properties. In *Composites Science and Technology*, ed. S. Adali, and V. Verijenko. University of Natal, South Africa, 1996, pp. 1–6.
15. Pêdzich, Z., Haberko, K., Piekarczyk, J., Faryna, M. and Litynska, L., Zirconia matrix-tungsten carbide particulate composites manufactured by hot-pressing technique. *Mater. Lett*. 1998, **36**, 70–75.
16. Haberko, K., Pêdzich, Z., Róg, G., Bucko, M. and Faryna, M., The TZP matrix-WC particulate composites. *Eur. J. Solid State Inorg. Chem.* 1995, **32**, 593–601.
17. Pêdzich, Z. and Haberko, K., Toughening mechanisms in the TZP–WC particulate composites. *Key Eng. Mater.* 1997, **132–136**, 2076–2079.
18. Anstis, G. R., Chantikul, P., Lawn, B. R. and Marshall, B. D., A critical evaluation of indentation techniques for measuring fracture toughness: I. Direct crack measurements. *J. Am. Ceram. Soc.* 1981, **64**, 533–558.
19. ASTM E 1876–99, *Am. Soc. Testing Mater.* 2000.
20. Toraya, H., Yoshimura, M. and Somiya, S., Calibration curve for quantitative analysis of the monoclinic-tetragonal ZrO_2 system by X-ray diffraction. *J. Am. Ceram. Soc*. 1984, **67**, C119–C121.
21. Basu, B., Vleugels, J. and Van der Biest, O., Toughness optimisation of ZrO_2–TiB_2 composites. *Key Eng. Mater.* 2002, **206–213**, 1170–1177.
22. Faryna, M., Haberko, K., Kozubowski, J. A. and Pêdzich, Z., Interphase boundary in the TZP–WC composites. *Electron Microsc.* 1998, **II**, 745–746.
23. Haberko, K., Pêdzich, Z., Piekarczyk, J. and Rog, G., Zirconia-tungsten carbide particulate composites. Part 1: manufacturing and physical properties. In *Basic Science—Trends in Emerging Materials and Applications*. Gruppo Editoriale Faenza Editrice, Faenza, 1995, pp. 29–36.
24. Stemmer, S., Vleugels, J. and Van der Biest, O., Transmission electron microscopy studies of interfaces in TiB_2–ZrO_2 composites. In *Interfacial Engineering for Optimised Properties*. *MRS Proceedings, Vol 458*. Materials Research Society, Warrendale, 1997, pp. 133–138.
25. Swain, M. V. and Rose, L. R. F., Strength limitations of transformation-toughened zirconia alloys. *J. Am. Ceram. Soc*. 1986, **69**, 511–518.
26. Faber, K. T. and Evans, A. G., Crack deflection processes—I. Theory. *Acta Metal.* 1983, **31**, 565–576.